Energy & Buildings 253 (2021) 111520

Contents lists available at ScienceDirect

Energy & Buildings

journal homepage: www.elsevier.com/locate/enb

Analytical solution for multi-borehole heat exchangers field including discontinuous and heterogeneous heat loads

T. Coen, B. François, P. Gerard *

Université Libre de Bruxelles (ULB), Building, Architecture and Town Planning Dept (BATir), Laboratoire de GéoMécanique, Avenue F.D. Roosevelt, 50- CPI 194/2, B-1050 Bruxelles, Belgium

ARTICLE INFO

Article history:
Received 2 August 2021
Revised 10 September 2021
Accepted 24 September 2021
Available online 1 October 2021

Keywords:
Shallow geothermal energy
Borehole heat exchanger
Multiple BHEs
Analytical solution
Heterogeneous thermal load
Hourly thermal load
Discontinuous heat extraction

ABSTRACT

Closed-loop borehole heat exchangers (BHEs) are used for heating/cooling buildings. For the sustainable design of these systems, analytical solutions provide fast and flexible tools to investigate the subsurface thermal response. In this study, from an existing analytical solution which predicts temperature field for discontinuous heat extraction/injection of multi-BHEs field, is improved to consider the case of heterogeneous heat loads (HHLs), i.e. heat loads tuned independently for each BHE to improve the long-term heat refurbishment in the subsurface. Also, we implemented the concept of BHE thermal resistance in order to determine the heat carrier fluid temperature. To provide accurate extreme temperatures, two aspects were analysed: the time step discretization; and the temporal resolution of thermal loads. The requirement for defining hourly thermal loads was demonstrated in order to properly predict extreme temperatures in the subsurface, as would be the case in an optimization problem of multi-BHEs with HHLs. As a study case, we showed the interest of HHLs to reduce localized thermal exhaustion of the geothermal system and to reduce extreme temperature variations and thermal drift in the most critical BHEs.

1. Introduction

Geothermal energy is a good alternative to produce electricity and especially for heating/cooling buildings [1]. Nowadays, several technologies are available to exploit this renewable energy [2]. Shallow geothermal energy (SGE) which is easily accessible and available worldwide and more specifically ground-coupled heat pumps (GCHPs) system are the most used [3,4]. A typical configuration of GCHPs involves borehole heat exchangers (BHEs). BHEs consists of a high-density polyethylene (HDPE) pipe where the heat carrier fluid circulates and a grout material that fills the borehole to maximize heat transfers and to seal the pipes. Depending on their geometry, BHE can be classified as follows: single U-pipe, double U-pipe and coaxial tubes. These types of vertical heat exchangers usually reach a depth of 50 m to 250 m and have a diameter of 10 cm to 15 cm [5]. For individual houses one BHE could be enough, but for larger buildings BHEs can be associated in parallel in order to compose a multi-BHEs field.

Accurately determining the temperature variation inside, in the near field and in the far field of BHEs depending on the energy extraction or injection, the hydro-thermal properties of the ground and the geometry of the multi-BHEs field is crucial. Indeed, it is important to ensure the regeneration of the thermal ground reservoir in order to guarantee the performance of these systems year after year. An irreversible drift of the ground temperature toward high or low values may significantly reduce the coefficient of performance of the heat pump, associated to the BHEs, for cooling or heating, respectively [6,7].

Consequently, in order to avoid the exhaustion of the ground heat source, it is of paramount importance to design the multi-BHEs field (i.e. number of BHEs and their depth) based on mathematical models that predict the temperature field in the BHEs (i.e. heat carrier fluid) and the surroundings (i.e. the ground) [8].

Since the early analytical model called Infinite Line Source (ILS) model presented by Ingersoll & Plass [9] in 1948, many analytical and numerical methods and solutions have been developed to study heat transfers between BHEs and ground, for single or multi-BHEs fields. Using the work of Carslaw & Jaespar [10], Ingersoll et al. [11] introduced the Infinite Cylindrical Source (ICS) model. These first models ignore the end effect, also called axial effects, of the BHE. Therefore, Eskilson [12] and then Zeng et al. [13] developed the Finite Line Source (FLS) model, more appropriate for studying the long-term performance of BHEs [14]. These analytical solutions are commonly used in practice because they are easy to implement, computationally fast and offer greater flexibility for parameterized design. However, these pioneer analytical

* Corresponding author.
E-mail address: Gerard.Pierre@ulb.be (P. Gerard).

https://doi.org/10.1016/j.enbuild.2021.111520
0378-7788/

Nomenclature

Nomenclature c	specific heat capacity J kg^{-1} K^{-1}
D	shank spacing m
$f(x,y,z,t)$	temperature response function mKW^{-1} s^{-1}
H	borehole length m
L	spacing between BHEs m
Nu	Nusselt number -
qL	heat flux per unit length Wm^{-1}
$qL(t)$	heat extraction function Wm^{-1}
R_b	borehole thermal resistance KmW^{-1}
r	radius m
r_pi	inner pipe radius m
r_po	outer pipe radius m
s	volumetric heat source Wm^{-3}
T	temperature K
T_0	undisturbed ground temperature K
T_b	temperature at the borehole wall K
T_f	temperature of the heat carrier fluid K
t	time s
Δt	time step discretization s
v	volumetric flow rate m3 s^{-1}
x, y, z	space coordinates m

Greek symbols

α	heat transfer coefficient Wm^{-2} K^{-1}
β	total number of BHEs -
λ	thermal conductivity Wm^{-1} K^{-1}
μ	dynamic viscosity Pa s
π	geometrical value -
ψ	density kgm^{-3}

Subscripts

av	average
b	borehole
f	heat carrier fluid
j	j th BHE
m	porous medium, ground
p	pipe
w	water

models are based on strong assumptions such as purely conductive heat transfer, continuous heat loads, uniform initial temperature, etc. which have led researchers to create more realistic models since the 2000s. Lamarche & Beauchamp [15] and Marcotte & Pasquier [16] developed a solution for the modelling of a BHE for a short time transient response. Bandos et al. [17] presented a new FLS model that considers the geothermal gradient effect and the temperature changes at the soil surface. Wagner et al. [18] and Erol et al. [19] have worked on a solution that takes into account groundwater flows based on the moving line source theory, initially proposed by Molina Giraldo et al. [20]. Erol et al. [19] also presented an analytical solution of discontinuous heat extraction both for single and multi-BHE field. Erol & François [21] as well as Hu [22] studied the heterogeneity of the subsoil and proposed an analytical solution considering a multiple sub-layer soil with different thermal properties.

Alternatively, with the rise of computers and numerical methods, numerical models have emerged for the simulation of BHEs (see [23–25], among others). They allow considering more complex configurations including multi-physical processes (conduction, convection, advection, etc.) [26], complex BHE geometries [27,28], ground heterogeneities [29] or irregular multi-BHEs field grid [30]. The counterpart being an important computing time and a long implementation procedure. Cui et al. [31] made a comprehensive review of the existing 2D and 3D models. All those studies, regardless of whether they are analytical or numerical, have highlighted the necessity to consider discontinuous heat loads if the aim is to capture the extreme temperatures in BHEs for design purposes.

In the studies presented above, it is also always assumed that the heat load is the same for all BHEs composing a multi-BHEs field (i.e. homogeneous heat load). However, Yu et al. [32] have shown that heterogeneous heat loads (i.e. heat loads can be tuned independently in each BHE) are more effective to ensure thermal regeneration of the ground. de Paly et al. [33] developed optimization procedure based on an analytical solution which regulated energy extraction for each single BHE of a system in order to minimize the maximum temperature change in the subsurface using linear programming. Beck et al. [34] used the same methodologies to define the best geometric arrangement and operation mode adjustment of a multi-BHEs field with heterogeneous heat loads. Retkowski et al. [35] confronted an analytical and numerical approach to a 16-borehole system with individual borehole specific heat extraction rates. However these literature review highlights the scarcity of development of models where heterogeneous heat loads can be considered, i.e. thermal loads that can be tuned independently in each BHE. In addition, all these studies only consider monthly heat loads while such coarse time resolution of the heat load is probably not sufficient to provide accurate estimations of the extreme temperatures, especially in the pipes and the near-field where the reactivity of temperature variations requires a smaller time resolution of the heat load.

In this study, we start from an existing analytical solution [19] which predicts temperature field for (i) discontinuous heat extraction/injection of (ii) multi-BHEs field and we improve it by incorporating the possibility to consider (iii) heterogeneous heat extraction/injection loads, i.e. different heat loads for each BHE of a multi-BHEs field. For that purpose, we first implement the concept of thermal resistance of the BHE, R_b, in order to determine the heat carrier fluid temperature evolution inside the BHEs. Secondly, the model equations are reorganized to consider heterogeneous heat loads. In order to provide accurate temperatures, two specific aspects are then analysed. First the discretization of the time step is optimized in order to obtain the best compromise between accurate determination of temperatures and calculation time. Then the temporal resolution of the thermal loads is investigated. The requirement for defining hourly thermal loads is demonstrated if accurate determination of the extreme temperatures is needed, as would be the case in an optimization problem of multiple BHEs with heterogeneous heat loads. Finally, the possibilities offered by our analytical solution which takes into account hourly and heterogeneous thermal loads are illustrated through a case study.

2. Mathematical model

As mentioned above, Erol et al. [19] have proposed an analytical solution taking into account groundwater flows and discontinuous heat extraction/injection for both single and multi-BHEs field. Current developments start from this original model, the basic equations of which being summarized in the following section for the sake of clarity. For more completeness, full details can be found in the original paper [19].

2.1. Temperature in the ground for homogeneous thermal load

The heat transfer problem which takes into account conduction of heat is governed by the following equation:

$$\rho_m c_m \frac{\partial^2 T}{\partial t} = \lambda_m \left(\frac{\partial^2 T}{\partial x^2} + \frac{\partial^2 T}{\partial y^2} + \frac{\partial^2 T}{\partial z^2} \right) + s \quad (1)$$

where $\rho_m c_m$ is the volumetric heat capacity of the porous medium, λ_m is the thermal conductivity of the porous medium and s is a volumetric heat source.

Starting from a Green's function, Erol et al. developed the solution to the partial differential Eq. (1) for a multi-BHEs field taking into account the axial effect:

$$f(x,y,z,t) = \sum_{j=1}^{\beta} \frac{1}{8\pi t \lambda_m} exp\left[-\frac{(x-x_j)^2}{\frac{4\lambda_m t}{\rho_m c_m}} - \frac{(y-y_j)^2}{\frac{4\lambda_m t}{\rho_m c_m}} \right] \overbrace{\left[erf\left(\frac{z}{\sqrt{\frac{4\lambda_m t}{\rho_m c_m}}} \right) - erf\left(\frac{z-H}{\sqrt{\frac{4\lambda_m t}{\rho_m c_m}}} \right) \right]}^{\text{axial effect}} \quad (2)$$

where β is the number of BHEs, (x_j, y_j) is the coordinates of the jth borehole and H the borehole length. With reference to the G-function introduced by Eskilson [12], this analytical f-function is the temperature response function of the model which is obtained by the sum of the contributions of each individual BHE j. Indeed, physical and thermal properties of materials are considered as temperature independent. This assumption is commonly used since temperature variations are relatively small in BHE problems. Therefore, the principle of superposition can be applied.

In order to be able to consider discontinuous heat extraction or injection, which is the case in practice for cooling or heating buildings, Erol et al. used convolution between the heat extraction function $q_L(t)$ and the f-function. This mathematical operation leads to the determination of the temperature difference, ΔT, at the location (x,y,z) as follows:

$$\Delta T(x,y,z,t) = \int_{-\infty}^{\infty} q_L(\tau) f(x,y,z,t-\tau) d\tau = \sum_{i=1}^{n-1} q_L(i\Delta t) f(x,y,z,t-i\Delta t)\Delta t \quad (3)$$

where n is the number of time steps. The convolution integral equation is discretized with a differential of Δt to be able to make an analytical evaluation.

By comparing this analytical solution with 3D-FEM models, Erol et al. demonstrated that this solution is able to provide temperature distribution around single and multi-BHEs for discontinuous heat extraction. In the following, in order to consider heterogeneous thermal loads, we improve the analytical model by implementing the effect of thermal borehole resistance, to predict the heat carrier fluid temperature (in the borehole pipe), and we optimize the discretization of the time step.

2.2. Heat carrier fluid temperature for homogeneous thermal load

In order to determine the heat carrier fluid temperature from the temperature at the borehole wall, T_b, calculated with Eq. (3), the work of Hellström [36] can be used. The mean temperature of heat carrier fluid, T_f, is obtained by:

$$T_f = T_b + R_b \cdot q_L \quad (4)$$

where T_b is the temperature at the borehole wall calculated with Eq. (3), R_b the fluid-to-ground thermal resistance and q_L the heat fluxes from the pipes. This relationship is only valid under the assumption of a steady-state heat flux in the borehole. This assumption is linked to the fact that R_b does not take into account the heat capacity of the borehole [15]. Eskilson [12] estimated the order of magnitude of the minimum time to reach this equilibrium state and showed that its order of magnitude is about one hour. This involves that the dynamic variation of the thermal load of less than one hour cannot be computed by the model presented here.

There are a number of methods to evaluate borehole thermal resistance [37] which can be analytical, empirical or even determined with in situ tests [38]. In this work, it was decided to use the analytical multipole method [39] limited to the first order for two typical BHE configurations, namely the single and the double U-pipe. This method has proven to be efficient and is implemented in well-known software for BHEs design such as EED [40]. Briefly, the mathematical developments for the two configurations are shown below with the parameters shown in Fig. 1.

Hellström [36] developed explicitly the first-order multipole approximation for single U-pipe BHE:

$$R_b(1) = \frac{1}{4\pi\lambda_b}\left[\beta + ln\left(\frac{r_b}{r_{po}}\right) + ln\left(\frac{r_b}{2D}\right) + \sigma ln\left(\frac{r_b^4}{r_b^4 - D^4}\right) - \frac{\frac{r_{po}^2}{4D^2}\left(1 - \sigma\frac{4D^4}{r_b^4 - D^4}\right)^2}{\frac{1+\beta}{1-\beta} + \frac{r_{po}^2}{4D^2}\left(1 + \sigma\frac{16D^4 r_b^4}{\left(r_b^4 - D^4\right)^2}\right)} \right] \quad (5)$$

where λ_b and λ_m are the thermal conductivities of the grout and the ground respectively, r_b and r_{po} are the borehole and the outer pipe radii respectively, D is the shank spacing, $\sigma = (\lambda_b - \lambda_m)/(\lambda_b + \lambda_m)$, $\beta = 2\pi\lambda_b R_p$ and R_p is the thermal resistance between the fluid and the material surrounding the pipe defined by:

$$R_p = \frac{1}{2\pi r_{pi}\alpha} + \frac{1}{2\pi\lambda_p} ln(r_{po}/r_{pi}) \quad (6)$$

where r_{pi} is the inner radius pipe, $\alpha = Nu\lambda_f/2r_{pi}$ and Nu is the dimensionless Nusselt number.

Claesson & Javed [41] developed explicitly the first-order multipole approximation for double U-pipe BHE:

$$R_b(1) = R_b(0) - \frac{1}{8\pi\lambda_b} \cdot \frac{b_1 \cdot p_{pc}\left(3 - 8\sigma \cdot p_c^4\right)^2}{1 + b_1 \cdot p_{pc}\left(5 + 64\sigma \cdot p_c^4 p_b^4\right)} \quad (7)$$

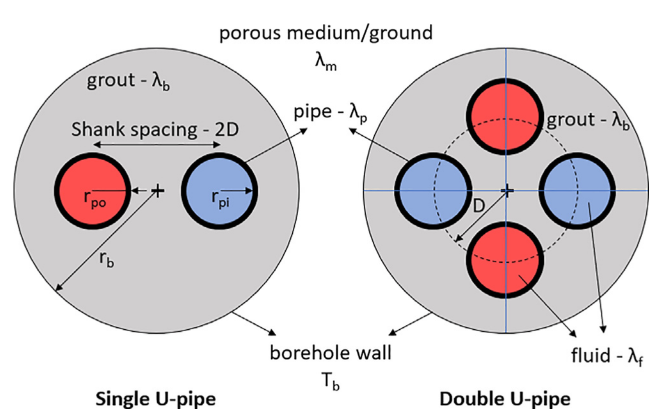

Fig. 1. Two typical BHE configurations with their associated geometrical (radius, r, and shank spacing, D) and thermal (thermal conductivity, λ) parameters.

where $p_{pc} = \frac{r_{po}^2}{4D^2}$, $p_c = \frac{D^2}{\sqrt[4]{r_b^8 - D^8}}$, $p_b = \frac{r_b^2}{\sqrt[4]{r_b^8 - D^8}}$, $b_1 = \frac{1-\beta}{1+\beta}$ and $R_b(0)$ is the zeroth-order multipole approximation defined by:

$$R_b(0) = \frac{R_p}{4} + \frac{1}{8\pi\lambda_b} \cdot \left[ln\left(\frac{r_b^4}{4r_{po}D^3}\right) + \sigma \cdot ln\left(\frac{r_b^8}{r_b^8 - D^8}\right)\right] \quad (8)$$

2.3. Ground and heat carrier fluid temperatures for heterogeneous thermal load

In most models that predict the temperature variation in heat carrier fluid and ground around BHE, it is usually assumed that the heat load is similar in each borehole of the multi-BHEs field. Therefore, with those models, it is not possible to investigate scenarios where heat loads vary according to the BHEs. However, these situations can have a positive effect on the regeneration of the thermal reservoir and avoid a decrease of the system performance.

The modifications made to the analytical solution consist in defining a temperature response function f_j and a heat extraction function q_{Lj} for each BHE j of the system. In this way, the thermal loads are defined individually for each BHE. This modification implies an increase of the calculation time proportional to the number of BHEs of the system. Indeed, the superposition principle involving the β boreholes is now performed after the convolution product:

$$f_j(x,y,z,t) = \frac{1}{8\pi t\lambda_m} exp\left[-\frac{(x-x_j)^2}{\frac{4\lambda_m t}{\rho_m c_m}} - \frac{(y-y_j)^2}{\frac{4\lambda_m t}{\rho_m c_m}}\right] \times \left[erf\left(\frac{z}{\sqrt{\frac{4\lambda_m t}{\rho_m c_m}}}\right) - erf\left(\frac{z-H}{\sqrt{\frac{4\lambda_m t}{\rho_m c_m}}}\right)\right] \quad (9)$$

$$\Delta T(x,y,z,t) = \sum_{j=1}^{\beta}\int_{-\infty}^{\infty} q_{Lj}(\tau) f_j(x,y,z,t-\tau)d\tau = \sum_{j=1}^{\beta}\sum_{i=1}^{n-1} q_{Lj}(i\Delta t) f_j(x,y,z,t-i\Delta t)\Delta t \quad (10)$$

2.4. Time step optimization

The implementation of heterogeneous thermal load increases the calculation time. It is therefore necessary to optimize the time step discretization, Δt, involved in Eq. (10). The time step should be chosen in order to reduce the calculation time but also to avoid discretization errors. Indeed, defining a very small time step improves the accuracy of the solution but also increases significantly the resolution time. On the other hand, too large time steps can lead to inaccurate temperatures. In practice, both functions of Eq. (10) (i.e. $q_L(t)$ and f-function) must be correctly discretized.

Concerning the discretization of $q_L(t)$, the time step must be equal or smaller than the smallest period without variation of the thermal load. In this way, any variation in the heat load can be accurately discretized. Due to the steady-state heat flux assumption in the implementation of the fluid-to-ground thermal resistance, R_b, it was determined that the variation of the thermal load could not be less than one hour. As a result, in the most critical situation, the time step discretization will be a maximum of one hour.

Since the f-function (Eqs. (2) and (9)) defines the thermal response of the analytical model it must be accurately discretized. The sensitivity analysis showed that this function has strong variations when evaluated close to the heat source (i.e. at the borehole walls), especially upon high thermal conductivity of the ground.

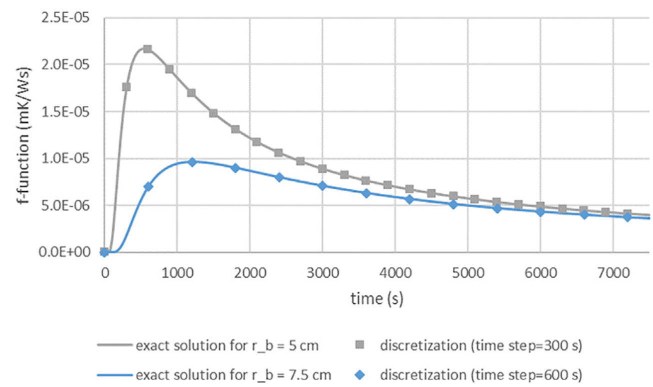

Fig. 2. Discretization of the f-function at the borehole wall for two single BHE of different radii, r_b ($\lambda_m = 2.5\ W/mK$).

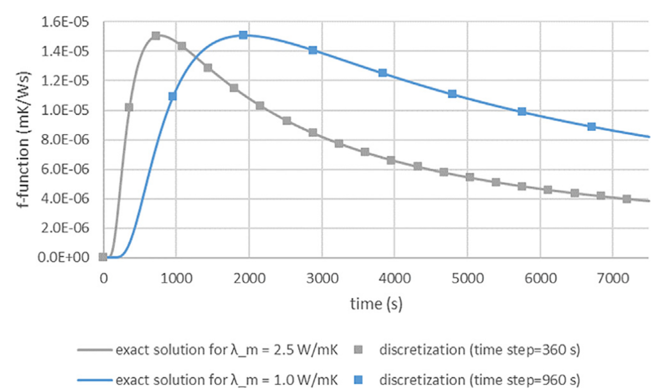

Fig. 3. Discretization of the f-function at the borehole wall of a single BHE for two different ground thermal conductivities, λ_m ($r_b = 0.06\ m$).

As can be seen in Figs. 2 and 3 for various ground thermal conductivities and borehole radii for a single BHE, the thermal response at the borehole wall consists of a fast-increasing phase, a maximum and then a relatively slow decreasing phase. This behaviour is identical at greater distances from the borehole but the amplitude is reduced and the maximum is reached at a much longer time. This is consistent with the fact that in the far field, thermal load is lower and the thermal plume takes longer to arrive.

The adopted methodology for the discretization of the f-function is to divide the increasing phase of this function in at least two time steps. In practice, the time corresponding to the maximum of the f-function can be easily determined analytically from Eqs. (2) and (9). This procedure illustrated in Figs. 2 and 3 shows that to correctly discretize the f-function the time step is between 5 and 16 min for typical values of the radius of BHE, r_b, and ground thermal conductivity, λ_m, when one considers the variation of temperature at the borehole wall.

In the end, the time step adopted is the minimum between the time step related to the thermal load and to the f-function.

3. Validation of the analytical solution

EED software has been chosen for the validation of the analytical solution in the case of multi-BHEs field with homogeneous thermal loads, since it is one of the most common and reliable geothermal tools used by the industry. EED is used for practical application in the design of BHE installations. Among other things, this software allows determining the heat carrier fluid temperature, T_f, inside the pipe at half the depth of the borehole. In case of multi-BHEs field, the software provides the average heat carrier fluid temperature, $T_{f,av}$, which is defined as the average fluid temperature between the β BHEs, at half the depth of the boreholes. The validity of EED average temperature results has been demonstrated several times using finite element numerical simulations [42].

The validation is done using a case study inspired from the "tutorial examples for EED v4" [43]. The practical example is a large office building with hourly simulation (i.e. the thermal load changes every hour). It consists of a multi-BHEs field of 25 boreholes with a regular grid of 5 x 5 BHEs and a spacing of 6 m between them. Parameters of the case study are shown in Table 1. The heating and cooling loads are shown in Fig. 4. The total heat load is slightly unbalanced in favour of heat extraction. For the validation, and to be able to compare the obtained results with the results from EED, an identical thermal load is applied to each BHE.

The objective being to validate the thermal response function f proposed by Erol et al. and its time discretization, as well as the implementation of the thermal resistance R_b, the simulations are carried out over a period of one year and the average temperature of the fluid $T_{f,av}$ are compared. It should be noted that the case of individual heat loads per BHE is not considered here but will be addressed in the next section, as an extension of the study.

Since EED only provides an average fluid temperature of all BHEs, the average fluid temperature is obtained from Eq. (4) using the borehole wall temperature averaged between each BHE:

$$T_{f,av} = T_{b,av} + R_b \cdot q_L \tag{11}$$

with

$$T_{b,av} = \text{average}(T_{b,j}) \tag{12}$$

where j refers to all BHEs of the system. By defining this, the comparison between the models and EED can be made. The average fluid temperature at half the depth of the 25 BHEs provided by EED and by the analytical solution are shown in Fig. 5. These results are more than satisfactory and show the accuracy of the analytical solution developed in this work for the prediction of fluid temperature in a multi-BHEs fields and for discontinuous heat loads, identical for each BHE (i.e. homogeneous heat loads).

Table 1
Parameters of the case study used for the validation of the analytical model.

Parameter	Symbol	Value	Unit
Borehole heat exchanger			
Type	–	double U-pipe	–
Configuration	M x N	5 x 5 (25)	BHEs
Spacing	L	6	m
Depth	H	120	m
Borehole radius	r_b	76.2	mm
Grout thermal conductivity	λ_b	1.6	W/mK
Outer pipe radius	r_{po}	16	mm
Inner pipe radius	r_{pi}	13	mm
Pipe thermal conductivity	λ_p	0.42	W/mK
Shank spacing	$2D$	60.4	mm
Heat carrier fluid			
Fluid thermal conductivity	λ_f	0.48	W/mK
Specific heat capacity	c_f	3795	J/kgK
Density	ρ_f	1052	kg/m^3
Viscosity	μ_f	0.0052	Pa s
Volumetric flow rate per borehole	v_f	0.48	l/s
Ground properties			
Undisturbed ground temperature	T_0	11.2	°C
Volumetric heat capacity	$\rho_m c_m$	2.20	MJ/m^{3}K
Ground thermal conductivity	λ_m	2.9	W/mK

Through this case study, the analytical model has proven to be effective in determining the evolution of the average fluid temperature with hourly simulations. In addition, the analytical model allows determining the fluid temperature specific to a BHE. Thus the extreme temperatures of the system, which can sometimes be noticeably different from the average temperature, can be defined. These results demonstrate that the analytical solution can be used for practical applications as the analysis of existing project monitoring data.

4. Result and discussion

This section highlights the new insights provided by the analytical solution for multi-BHEs field. For that purpose, the case study presented in the previous section is considered.

4.1. Temporal resolution of the heat load profile

The models taking into account heterogeneous thermal loads found in the literature are limited to monthly simulations. This coarse temporal resolution of the heat load can have a relatively strong impact on the results as it will be shown in this section.

Based on the load case presented in Fig. 4, three simulations have been carried out with hourly, weekly and monthly homogeneous thermal loads. The results shown in Fig. 6 illustrate the average fluid temperature evolution of these three load cases. It can be noticed that the thermal amplitude:

$$max(T_{f,av}(t)) - min(T_{f,av}(t)) \quad \text{for} \quad t \in (0 - 365)\ \text{days} \tag{13}$$

strongly depends on the type of loading. It goes from 20.5 °C for an hourly simulation to 10.6 °C for a monthly simulation. The more thermal load is averaged over a long period of time, the smoother the peaks loads will be. A monthly load therefore gives the general evolution of the temperature without determining the exact extreme temperatures that the fluid reaches. The monthly load could probably be used to evaluate the possible drift of mean temperature year after year (in case of unbalanced thermal loading over the year) but cannot be used to provide most critical temperature variation upon peak demand.

Furthermore, it can be seen that when the temporal resolution of the heat load is too low (i.e. monthly), the extreme temperatures (i.e. $T_{f,av,max}(t)$ and $T_{f,av,min}(t)$) do not coincide with those of more detailed simulations. A monthly simulation cannot therefore determine with sufficient accuracy the period when temperature fluctuations are most significant.

Those results highlight the importance of using an analytical solution able to predict the heat carrier fluid temperature from hourly thermal loading. Moreover, during the design phase of a geothermal system, determining with accuracy the hourly (dynamic) thermal needs of the buildings seems to be a key element to improve the accuracy of the temperature predictions.

4.2. Temperature evolution of each specific BHE

As mentioned earlier, the majority of the existing solutions, including EED, provide the average temperature of the fluid in the entire considered system. These results are interesting because usually a collector unifies the heat carrier fluids coming from each BHE in a single pipe (with averaged temperature) before the heat pump. To obtain the inlet temperature to the heat pump, the averaged temperature is sufficient. However, a result limited to the average temperature of the heat carrier fluid does not allow analysing the thermal behaviour of each individual BHE. Nevertheless, it has been shown [33,44] that the thermal exhaustion can be concentrated in a certain area of the BHEs field. It is therefore interesting to

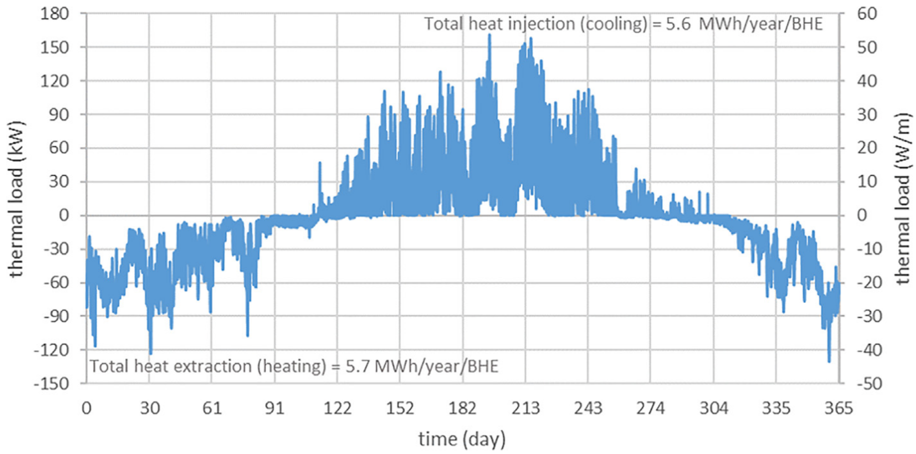

Fig. 4. Hourly and homogeneous thermal loads for 365 days of the case study. Positive values indicate heat injection and negative values indicate heat extraction.

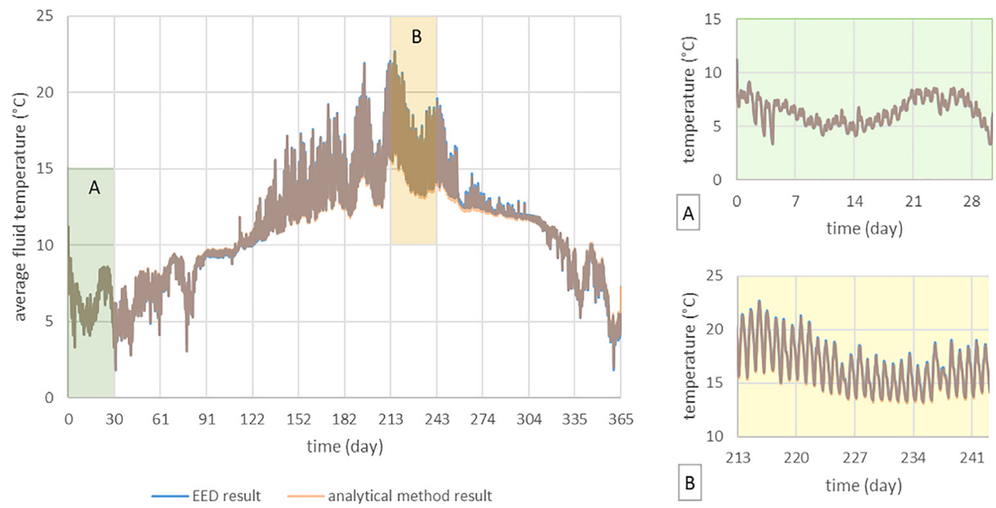

Fig. 5. Case study: average fluid temperature inside the 25 BHEs at the half depth provided by EED and the analytical model for hourly homogeneous heat loads.

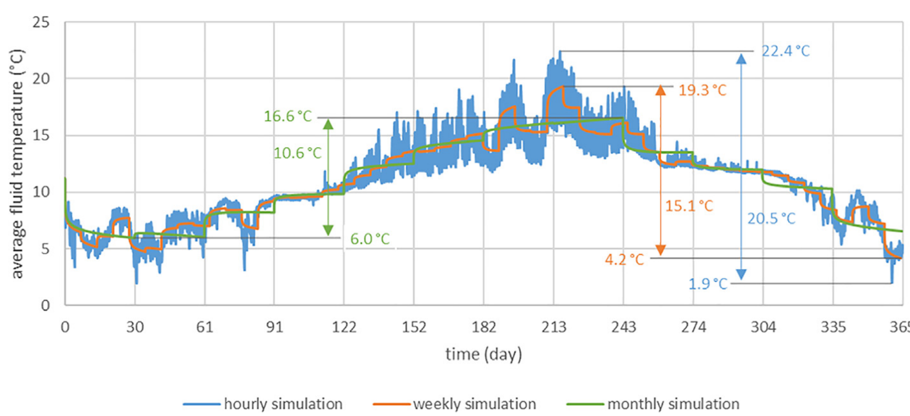

Fig. 6. Average fluid temperature inside the 25 BHEs at the half depth provided by the analytical model for three different temporal resolutions of the thermal load, annual thermal amplitude ($T_{f,av,max}(t) - T_{f,av,min}(t)$) is given for each load case.

develop a modular solution that can provide both the average fluid temperature and the temperature of the heat carrier fluid in a specific BHE.

To illustrate the relevance of having access to the heat carrier fluid of a specific BHE a geothermal system with a strongly unbalanced thermal load is used. For that purpose, we restart from the previously presented study case and its homogeneous thermal load (Fig. 4), but we remove the heat injection, only keeping homogeneous heat extraction (i.e. similar heat extraction for each BHE). Fig. 7 shows the comparison between the average fluid temperature and the temperature evolution of the most peripheral (I) and the most central (II) BHE (see BHEs configuration in Fig. 8).

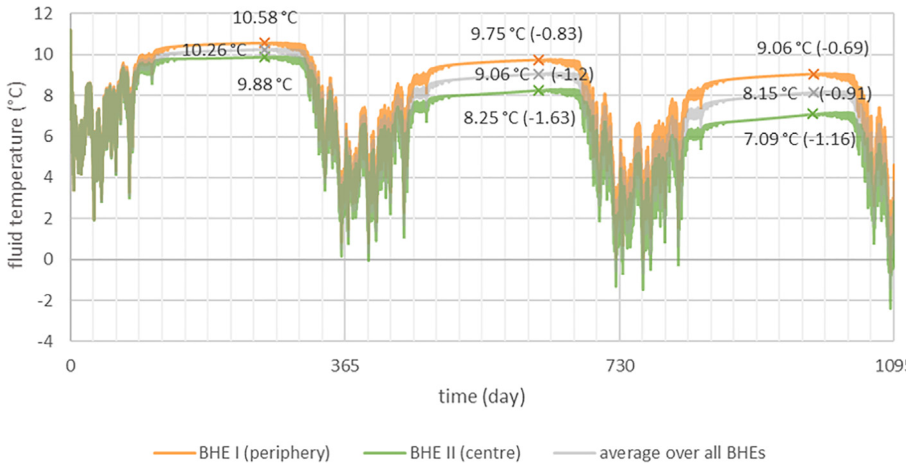

Fig. 7. Comparison of the temperature evolution of two specific BHEs and the average value of the system for a homogeneous purely extraction heat load case, thermal drift is defined from the temperature of the day 258 (mid-September) of each year and the number in bracket reports the variation of temperature over the last year.

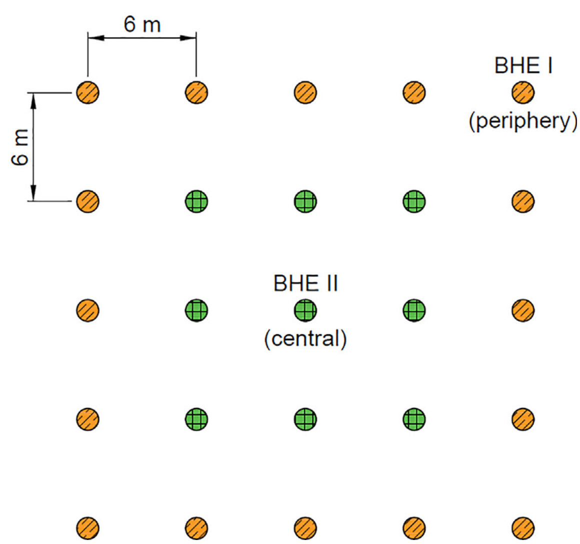

Fig. 8. Layout of the 25 BHEs with spacing of 6 m. The field is distinguished by 16 peripheral BHEs, which are used all year round, and 9 central BHEs, which are used during high heat extraction (>45 kW).

The calculation was made over 3 years. In line with the fact that the heat load is unbalanced, a thermal drift is observed year after year. Indeed, since it is only a heat extraction, the ground is constantly cooling down, it does not have the possibility to regenerate itself and the ground temperatures are continuously decreasing year after year. The drift is defined by the temperature at the end of the summer period (mid-September, 258th day of the year) just before the autumn heat extraction starts. Since the drift is greater at the centre than at the periphery, this illustrates the greater thermal exhaustion at the centre of the system. It can be observed that the thermal behaviour is specific to each BHE and relatively large differences can exist with respect to the average temperature.

This highlights the importance of focusing not only on average heat carrier fluid temperature but also on the specific thermal behaviour of each BHE. Indeed, a localized thermal exhaustion of the system may lead to a local freezing of the subsoil.

4.3. Heterogeneous thermal load

In case of unbalanced energy needs between heating and cooling, homogeneous thermal loading leads to non-uniform deterioration of the ground thermal storage. Indeed, it has been shown in the previous section that the centre of the system undergoes greater temperature variation. This observation motivated us to develop a solution capable of exploring situations where the thermal load would be heterogeneous and hourly.

Therefore, the developed analytical model allows now to impose a particular and independent hourly thermal load to each BHE or group of BHEs. The objective is to reduce the thermal drift and minimize the temperature variation in the most critical boreholes (usually in the centre of the BHEs field).

In order to illustrate the possibilities provided by the analytical solution, the geothermal system presented previously will be divided into two zones visible on Fig. 8. The first zone, consisting of the 16 peripheral BHEs, will be operated throughout the year, whereas the second zone, consisting of the 9 central BHEs, will only be activated when the thermal load is high. Fig. 9 shows the total thermal load applied to the geothermal system which corresponds to the initial load shown in Fig. 4 but without the cooling. When the thermal load is high (>45 kW) all BHEs are activated and each one receives the same thermal load. For low heat extraction (<45 kW), only peripheral BHEs are used. This threshold corresponds to 30% of the maximum value of the thermal load. The consequence of this heterogeneous heat load is that the peripheral BHEs extract almost twice as much energy per year as the central boreholes (i.e. 6.8 and 3.8 MWh/year/BHE respectively). The homogeneous case extracts 5.7 MWh/year/BHE.

The analysis will focus on the temperature evolution of two BHE-named BHE I and II- representing respectively the peripheral and central zone under homogeneous and heterogeneous thermal load. The simulation is carried out over 10 years, with the ground and GHE properties defined in Table 1. An initially homogeneous ground temperature is thus considered for the case study with heterogeneous heat loads.

Fig. 10 shows the fluid temperature of the two BHEs of interest during the tenth year of simulation. For the peripheral BHE I in a general way the heterogeneous thermal load slightly degrades the temperature, especially during periods of low heat extraction because the thermal load is concentrated to the peripheral BHEs. This degradation is logical because the heterogeneous thermal load configuration demands more to the peripheral BHEs. However, this is to favour the central BHEs where, for the central borehole II, with a reduced annual thermal load, a relatively good improvement is noticeable. For each year two remarkable values are defined at both BHEs (I and II): the temperature at mid-September (thermal drift) and the minimum temperature. After ten years,

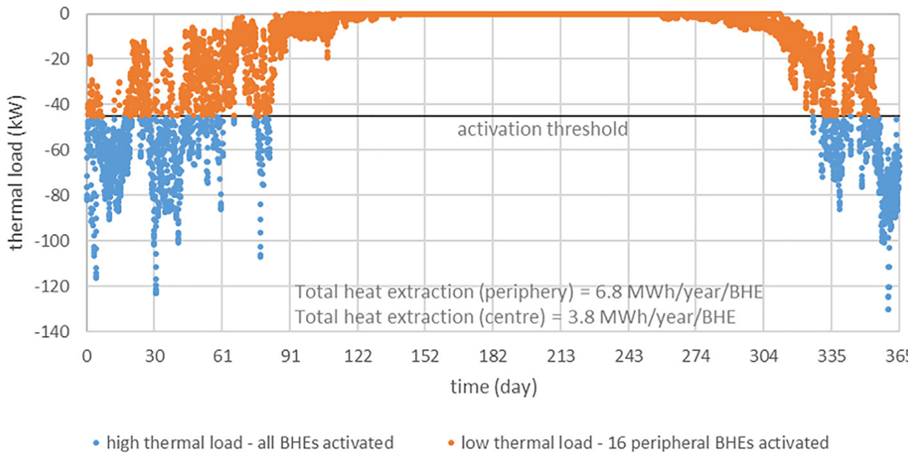

Fig. 9. Heterogeneous hourly thermal loads (only extraction) applied to the periphery and central BHEs. All the BHEs are activated when the total extraction is higher than 45 kW. Otherwise only the peripheral BHEs are used.

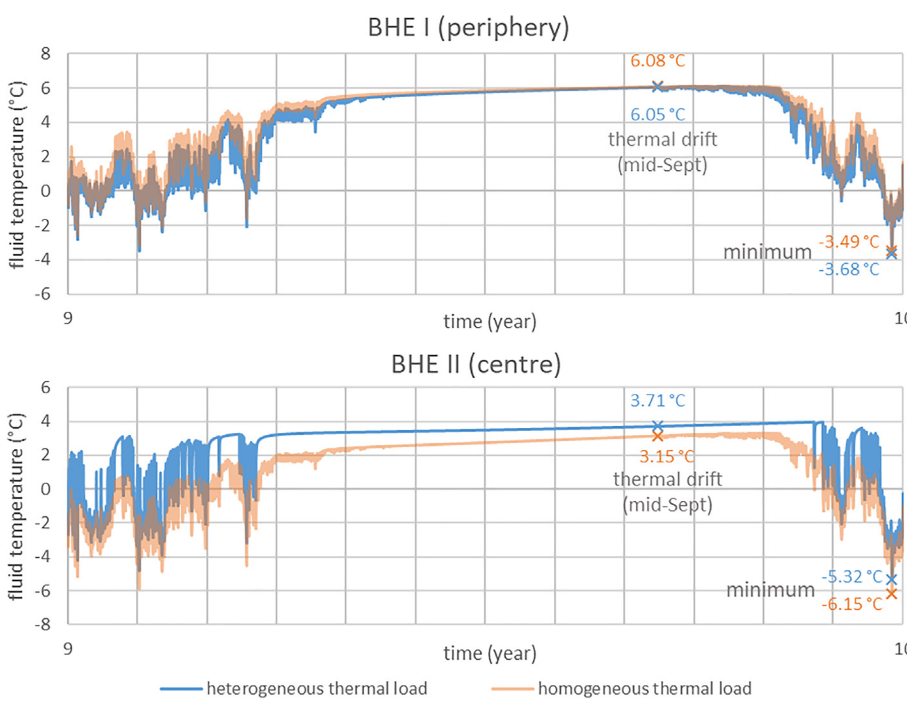

Fig. 10. Fluid temperature for the tenth year of simulation for two particular BHEs with two different thermal loading strategies. Two particular temperatures are defined each year, namely the temperature of the thermal drift and of the minimum.

heterogeneous thermal loading degrades these two temperatures by 0.03 °C and 0.19 °C respectively for BHE I and improves by 0.56 °C and 0.82 °C for BHE II.

These remarkable temperatures which give the annual tendency of the temperature evolution are plotted in Fig. 11(a) and (b) for the first 10 years of the simulation. Since the load is unbalanced, these temperatures are continuously deteriorating. Furthermore, it can be seen that even though the heat extraction in the centre (BHE II) is reduced, the temperature deterioration is still higher than in BHE I. However, the heterogeneous strategy slightly deteriorates both the minimum temperature and the thermal drift for the peripheral BHE I. This deterioration occurs mainly during the first year, after which the deterioration hardly changes at all. For the central BHE II there is a continuous improvement of these remarkable temperatures in comparison to a homogeneous strategy during the 10 years of the simulations.

Although the thermal load on the peripheric BHEs has increased with heterogeneous thermal load, Fig. 11(c) shows that the degradation of the remarkable temperatures is only slightly different compared to the noticeable improvement in the centre of the system. Moreover, the differences between the temperatures due to the different strategies remain almost constant from the first year for the peripheral probe I, while for the central BHE II this difference increases from year to year and only stabilizes in the long term.

It can be concluded that, with heterogeneous thermal load, the local deterioration of the thermal reservoir in the centre of the system is reduced. In addition, this type of optimization with

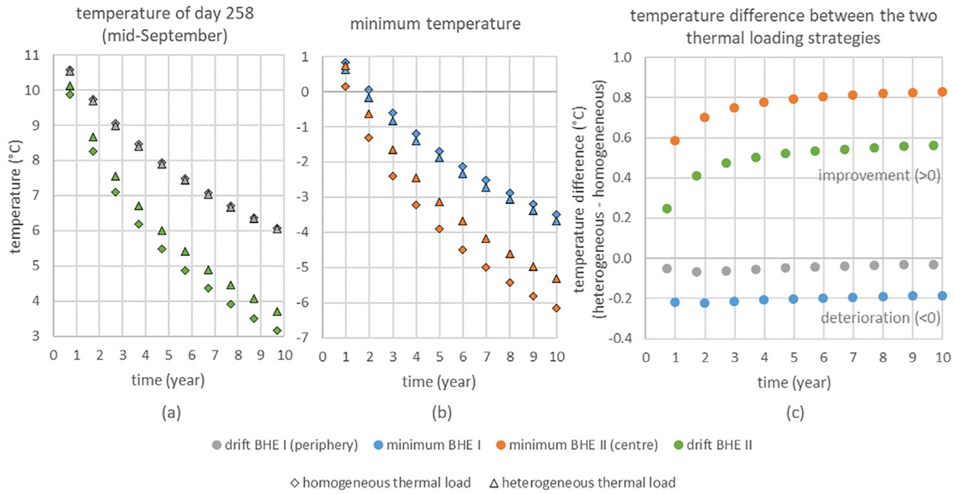

Fig. 11. Annual remarkable values ((a) of day 258 (thermal drift) and (b) minimum temperature) for two particular BHEs with two different thermal loading strategies (homogeneous and heterogeneous thermal load) and (c) comparison of the influence of these two strategies on the temperature evolution. Heterogeneous thermal loading improves thermal drift and minimum temperature for the central BHE II and slightly deteriorates these values for the peripheral BHE I.

heterogeneous thermal load only makes sense in the long term, as the improvement is even more marked after a few years.

5. Conclusion

Starting from the analytical solution developed by Erol et al. [19] that provides temperature distribution around single and multi-BHEs for discontinuous heat extraction/injection, we have incorporated the possibility to consider heterogeneous heat loads, i.e. different heat loads for each BHE of a multi-BHEs field. The model equations have been reorganized to take into account a specific and independent heat load at each BHE or group of BHEs. This new feature allows to optimize the distribution of thermal demands on each individual BHE in order to mitigate the non-uniform deterioration of the ground thermal storage and the localized thermal exhaustion of the system.

Also, the need to predict the temperature in the heat carrier fluid (in addition to the temperature field in the ground) led us to implement the concept of thermal resistance of the BHE, R_b, determined analytically for two typical BHE configurations, namely single and double U-pipe.

By modelling a real 5 $\times$ 5 borehole heat exchanger field submitted to discontinuous heat extraction and injection over one annual cycle, we have investigated several temporal resolution of the thermal load and we have shown that an heat load discretized by hour is required to accurately determine the critical temperature variation and especially to determine when these temperatures are reached.

Finally, the developed analytical solution has been used on the 5 $\times$ 5 multi-BHE field with hourly and heterogeneous thermal load where central BHEs are only used during high extraction demand. The results showed that such a thermal load distribution between BHE allows reducing the thermal drift and limiting the temperature drop during peak demand in the central BHE without significantly impacting the temperature evolution of the peripheral boreholes.

This developed analytical solution provides an efficient tool for the design of multi BHEs, considering discontinuous and heterogeneous thermal load. The main limitation is related to the assumption of ground homogeneity. Multi-layered ground is not considered here, even if the work of Erol and François [21] provides a method to consider it in future developments. Also, the tool is particularly well-adapted to calculate temperature in a limited number of locations. However, the prediction of temperature map in a large domain, that requires many calculated points, may lead to important computational time.

For further investigations and perspectives, a comparison with numerical models could be interesting. Also, this flexible and modular analytical solution can be combined with specific optimization approaches to reduce the exhaustion of the system and to realize more sustainable design. In addition, the study of the impact of groundwater flows can be carried out quite easily by slightly modifying the equations based on the work of Erol et al. [19].

Declaration of Competing Interest

The authors declare that they have no known competing financial interests or personal relationships that could have appeared to influence the work reported in this paper.

Acknowledgements

This work was supported by the European Regional Development Fund (EDRF) and the Brussels-Capital Region in the frame of the project "Brugeo".

References

[1] J. Lund, A. Toth, Direct utilization of geothermal energy 2020 worldwide review, Geothermics 90 (2021) 101915.
[2] E. Barbier, Geothermal energy technology and current status: an overview, Renewable and Sustainable Energy Reviews 6 (2002) 3–65.
[3] B. Sanner, C. Karytsas, D. Mendrinos, L. Rybach, Current status of ground source heat pumps and underground thermal energy storage in Europe, Geothermics 32 (2003) 579–588.
[4] G. Florides, S. Kalogirou, Ground heat exchangers–A review of systems, models and applications, Renewable Energy 32 (2007) 2461–2478.
[5] A. Mustafa Omer, Ground-source heat pumps systems and applications, Renewable and Sustainable Energy Reviews, 12, 2008, pp. 344–371.
[6] E. Atam, L. Helsen, Ground-coupled heat pumps: Part 2–literature review and research challenges in optimal design, Renewable and Sustainable Energy Reviews 54 (2016) 1668–1684.
[7] L. Aresti, P. Christodoulides, G. Florides, A review of the design aspects of ground heat exchangers, Renewable and Sustainable Energy Reviews 92 (2018) 757–773.
[8] M. Ahmadfard, M. Bernier, A review of vertical ground heat exchanger sizing tools including an inter-model comparison, Renewable and Sustainable Energy Reviews 110 (2019) 247–265.
[9] L. Ingersoll, H. Plass, Theory of the ground pipe heat source for the heat pump, vol. 20, Piping and Air-Conditioning, 1948.
[10] H. Carslaw, J. Jaeger, Conduction of Heat in Solids, Clarendon Press, Oxford, 1947.

[11] L. Ingersoll, O. Zobel, A. Ingersoll, Heat Conduction With Engineering, Geolofical and Other Application, McGraw-Hill, New-York, NY, USA, 1954.
[12] P. Eskilson, Thermal analysis of heat extraction boreholes, Ph.D. thesis, University of Lund, Sweden, 1987.
[13] H. Zeng, N. Diao, Z. Fang, A finite line-source model for boreholes in geothermal heat exchangers, Heat Transfer-Asian Research 31 (7) (2002) 558–567.
[14] M. Philippe, M. Bernier, D. Marchio, Validity ranges of three analytical solutions to heat transfer in the vicinity of single boreholes, Geothermics 38 (4) (2009) 407–413.
[15] L. Lamarche, B. Beauchamp, New solutions for the short-time analysis of geothermal vertical boreholes, International Journal of Heat and Mass Transfer 50 (2007) 1408–1419.
[16] D. Marcotte, P. Pasquier, Fast fluid and ground temperature computation for geothermal ground-loop heat exchanger systems, Geothermics 37 (2008) 651–665.
[17] T. Bandos, E. Montero, J. Fernández, J. Santander, J. Pérez Isidro, et al., Finite line-source model for borehole heat exchangers: effect of vertical temperature variations, Geothermics 38 (2009) 263–270.
[18] V. Wagner, P. Blum, M. Kübert, P. Bayer, Analytical approach to groundwater-influenced thermal response tests of grouted borehole heat exchangers, Geothermics 46 (2013) 22–31.
[19] S. Erol, M. Hashemi, B. François, Analytical solution of discontinuous heat extraction for sustainability and recovery aspects of borehole heat exchangers, International Journal of Thermal Sciences 88 (2015) 47–58.
[20] N. Molina-Giraldo, P. Blum, K. Zhu, P. Bayer, Z. Fang, A moving finite line source model to simulate borehole heat exchangers with groundwater advection, International Journal of Thermal Sciences 50 (2011) 2506–2513.
[21] S. Erol, B. Francois, Multilayer analytical model for vertical ground heat exchanger with groundwater flow, Geothermics 71 (2018) 294–305.
[22] J. Hu, An improved analytical model for vertical borehole ground heat exchanger with multiple-layer substrates and groundwater flow, Applied Energy 202 (2017) 537–549.
[23] I.I. Stylianou, S. Tassou, P. Christodoulides, L. Aresti, G. Florides, Modeling of vertical ground heat exchangers in the presence of groundwater flow and underground temperature gradient, Energy and Buildings 192 (2019) 15–30.
[24] D. Bauer, W. Heidemann, H. Diersch, Transient 3D analysis of borehole heat exchanger modeling, Geothermics 40 (2011) 250–260.
[25] T. Ozudogru, C. Olgun, A. Senol, 3D numerical modeling of vertical geothermal heat exchangers, Geothermics 51 (2014) 312–324.
[26] C. Li, P. Cleall, J. Mao, J. Muñoz-Criollo, Numerical simulation of ground source heat pump systems considering unsaturated soil properties and groundwater flow, Applied Thermal Engineering 139 (2018) 307–316.
[27] N. Makasis, G. Narsilio, I. Johnston, Ground-source heat pump systems: The effect of variable pipe separation in ground heat exchangers, Computers and Geotechnics 100 (2018) 97–109.
[28] B. Cerfontaine, G. Radioti, F. Collin, R. Charlier, Formulation of a 1D?nite element of heat exchanger for accurate modelling of the grouting behaviour: application to cyclic thermal loading, Renewable Energy 96.A (2016) 65–79.
[29] G. Brunetti, H. Saito, T. Saito, J. Šimunek, A computationally efficient pseudo-3D model for the numerical analysis of borehole heat exchangers, Applied Energy 208 (2017) 1113–1127.
[30] R. Al-Khoury, T. Kölbel, R. Schramedei, Efficient numerical modeling of borehole heat exchangers, Computers and Geosciences 36 (2010) 1301–1315.
[31] Y. Cui, J. Zhu, S. Twaha, S. Riffat, A comprehensive review on 2D and 3D models of vertical ground heat exchangers, Renewable and Sustainable Energy Reviews 94 (2018) 84–114.
[32] M. Yu, K. Zhang, X. Cao, A. Hu, P. Cui, Z. Fang, Zoning operation of multiple borehole ground heat exchangers to alleviate the ground thermal accumulation caused by unbalanced seasonal loads, Energy and Buildings 110 (2016) 345–352.
[33] M. de Paly, J. Hecht-Méndez, M. Beck, P. Blum, A. Zell, P. Bayer, Optimization of energy extraction for closed shallow geothermal systems using linear programming, Geothermics 43 (2012) 57–65.
[34] M. Beck, P. Bayer, M. de Paly, J. Hecht-Méndez, A. Zell, Geometric arrangement and operation mode adjustment in low-enthalpy geothermal borehole fields for heating, Energy 49 (2013) 434–443.
[35] W. Retkowski, G. Ziefle, J. Thöming, Evaluation of different heat extraction strategies for shallow vertical ground-source heat pump systems, Applied Energy 149 (2015) 259–271.
[36] G. Hellström, Ground Heat Storage: Thermal Analysis of Duct Storage Systems, Ph.D. thesis, Departement of Mathematic Physics, University of Lund, Lund, Sweden, 1991.
[37] L. Lamarche, S. Kajl, B. Beauchamp, A review of methods to evaluate borehole thermal resistances in geothermal heat-pump systems, Geothermics 39 (2) (2010) 187–200.
[38] D. Marcotte, P. Pasquier, On the estimation of thermal resistance in borehole thermal conductivity test, Renewable Energy 33 (11) (2008) 2407–2415.
[39] J. Bennet, J. Claesson, G. Hellström, Multipole method to compute the conductive heat flows to and between pipes in a composite cylinder, Tech. Rep. 3–1987, Departement of Building Physics, Lund Institute of Technology, Lund, Sweden, 1987.
[40] G. Hellström, B. Sanner, M. Klugescheid, T. Gonka, S. Mårtensson, Experiences with the borehole heat exchanger software eed, in: 7th International Conference on Thermal Energy Storage, Megastock '97, Sapporo, Japan, 1997, p. 7.
[41] J. Claesson, S. Javed, Explicit multipole formulas and thermal network models for calculating thermal resistances of double U-pipe borehole heat exchangers, Science and Technology for the Built Environment 25 (8) (2019) 980–992.
[42] G. Hellström, B. Sanner, PC-programs and modelling for borehole heat exchanger design, in: International Geothermal Days, Bad Urach, Germany, 2001, p. 10.
[43] Tutorial Examples for EED v4, Tech. rep., Buildingphysics.com (Jan. 2020). URL: https://buildingphysics.com/download/exampleseed.pdf.
[44] P. Bayer, M. de Paly, M. Beck, Strategic optimization of borehole heat exchanger field for seasonal geothermal heating and cooling, Applied Energy 136 (2014) 445–453.